

Analysis of grain size in MgO-Co multilayers using TEM investigations

I. MARIN^{a,*}, V. CIUPINA^a, G. PRODAN^a, I. M. OANCEA STANESCU^a

^aOvidius University of Constanta, 9000527, Constanta, Romania

Thermionic vacuum arc (TVA) is a growth technique among others (pulsed laser deposition, electron beam deposition, thermal evaporation) used in fabrication for solid-state electronic devices, sensing devices, information storage. Electrical and magnetical properties behaviour of thin films depends of grain size. An important characteristic of thin film technologies is the possibility to control the grain size. A few applications of the effect of the final mean grain size on the properties of thin films are spintronic devices. In TVA deposition there are different methods for controlling grain size including the distance between cathode and anode or the relativ position of the two electrodes. In this paper we present TEM (Philips CM 120 ST) analysis on MgO-Co multilayers prepared by TVA method, demonstrating the uniform distribution of the grains and their *nm*-scale as shown in the histogram.

(Received July 8, 2011; accepted June 6, 2012)

Keywords: Multilayers, Grain size, Feret diameter, TEM

1. Introduction

Multilayers are a category of the so-called nanostructured materials which are intensively studied and have important applications in many fields. These applications that take advantage of their significant properties include ultrahigh-strength materials, thermoelectric devices, coatings for gears and bearings, aircraft and automobile engines, cutting and machine tools, high-performance capacitors. Products incorporating multilayers promise less friction and wear, higher temperature operation, corrosion resistance, and low electrical resistivity. Multilayers made of metals get stronger and harder, while multilayer ceramics become less brittle [1-3].

In nanoparticle science, it is important to devise controlled ways for obtaining uniform nanoparticles – particles of 0,01 μm (10 nm), and smaller.

There are many approaches in formation of uniform nanoparticles in compounds, multilayers, solutions with many experimental and theoretical challenges. For properly selected experimental conditions, it is expected to observe a narrow size distributions of the synthesized nanomaterials. In production of multilayer materials we used a method called thermionic vacuum arc (TVA) and we analyzed the grain size of MgO-Co particles using a TEM (Philips CM 120 ST) with a resolution of 0,2 nm.

2. Experimental

2.1 Particle size distribution

The particle size distribution or grain size distribution of a nanomaterial is a list of values or a mathematical function that defines the relative amounts of particles present, sorted according to size [4-5]. The particle size

distribution of a material can be important in understanding its physical and chemical properties. It can change the electrical and magnetical properties, the reactivity of solids participating in chemical reactions. Therefore, needs to be tightly controlled in many industrial products, such as electronical devices.

To evaluate the particles diameter it can be used Feret diameter – the longest chord of the projection of the object at a specific angle. The Feret diameter, F , is defined as the perpendicular distance between parallel lines, tangent to the perimeter at opposite sides of a 2D object in a certain direction as shown in Fig. 1 [6-7].

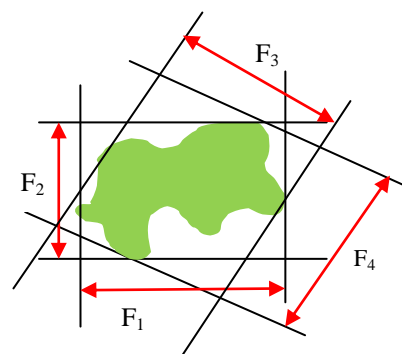


Fig. 1. Feret diameter.

When measuring the Feret diameter in several predetermined directions, the obtained maximum value is the maximum Feret diameter (Fig. 2). Minimum, maximum and average Feret diameter can be determined from a set of ferrets measured once every five degrees (5°).

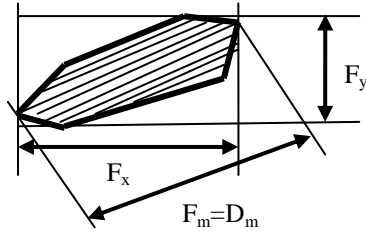


Fig. 2. Definition of Feret diameter in x direction (F_x), y direction (F_y), and maximum Feret diameter, F_m (maximum dimension, D_m).

For calculation the mean diameter of the particles was assumed a lognormal distribution of the experimental values. The particle size distribution was suitable to a lognormal function (eq.1):

$$y = y_0 + A \cdot \exp \left[-\frac{\ln^2(x/x_c)}{2w^2} \right] \quad (1)$$

where y_0 is a baseline, A a constant related to the number of particles analysed, x_c is the size of the distribution maximum, and w is correlated with the dispersion of the particle diameters [8-9].

2.2 Filling factor

The electrical conductance for the deposited nano-sized thin films depends on the filling factor of the connected and empty spaces.

At low filling factor, the particles may be separated individually. The mechanism of conductivity on the thin film can be extensively addressed by a simple tunneling between localized insulating states [10-11] that imply a high resistivity at low temperatures.

When the filling factor is large enough for the particles to collect into conglomerates, and conducting paths appear from one side of the sample to the other, the sample begins to exhibit conduction.

The electrical conductivity $\sigma(R, f, A)$ depends on the particle size R , the filling factor f , and the aggregation factor A , which represents the extent to which the particles are connected with each other to those are discrete. Potential barriers usually occur between the boundaries of particles to particles, therefore the conduction electrons will present grain boundary scattering.

The electron mean free path, l , within each particle being larger than the grain size, R , from simulation by the random process [12], deduce a semi-empirical law for the electrical conductivity (eq.2):

$$\sigma_g = \frac{ne^2l}{mv_f} \Gamma^{l/R} \quad (2)$$

within the grain boundary, where, Γ is the transmission probability for electrons to tunneling through the grain boundary, v_f is the Fermi velocity and l is the electron mean free path.

The grain boundary scattering as expressed in equation (2), required that the grain size must be larger than the electron mean free path. In metal particle the mean free path is determined by the electron phonon scattering.

Reducing the particle size further into nanosize, the experimental data on metallic nanoparticle films [13-14] composing of conglomerated nanoparticles giving rise to conductivity, indicate a linear Bloch-Grüneisen [15] for absorption or emission a phonon at high temperatures, which can be fitted successfully with an effective Debye temperature, θ_D . Debye temperature decreases as the particle size is reduced.

The resistivity measurements indicate anomalous behaviour occurring at the lower temperature end of the linear Bloch-Grüneisen plot. An explanation of this behaviour is the contribution of the Kondo effect resulting from spin flip-flop scattering of conduction electrons with the magnetic impurities in the sample.

When the bulk metal is dispersed into nanoparticles, each of them retained even or odd number of electrons with equal probabilities. The nanoparticles with unpaired spin behave as magnetic impurities which contribute to spin scattering. This behavior of spin-flip scattering determines a Kondo resistivity (eq.3):

$$\rho_{spin}(T) = \rho_1 - \rho_2 |J| \ln(T) \quad (3)$$

where, ρ_1 and ρ_2 are independent of temperature and J is the exchange integral between s and p electrons.

The particles occupied with odd number of electrons have a net electron spin and behave like paramagnetic impurities.

In Kondo theory about resistivity in nanoparticles is the assumption that the Kondo temperature, T_k decreases as the particle size is reduced according to:

$$T_k \approx T_{k0} e^{-R_0/R} \quad (4)$$

where, T_{k0} is for bulk value and R_0 is a constant.

From the equation $T_k \rightarrow 0$ when $R \rightarrow 0$ and $T_k \rightarrow T_{k0}$ when the particle size approaches the bulk solid dimension.

The particle size distribution is under the assumption of a log-Gaussian curve and a statistical function $f(T_k)$ is introduced to employ the distribution of T_k due to different particle size being presumed to be the same form as the particle size distribution (eq.5):

$$f(T_k) = \frac{1}{\sqrt{2\pi}} \frac{1}{\ln \sigma_k} \frac{1}{T_k} \exp \left\{ -\left(\frac{\ln T_k / T_k}{\sqrt{2 \ln \sigma_k}} \right)^2 \right\} \quad (5)$$

Considering all this terms, the total resistivity $\rho_{total}(T)$ will be given by (eq.6):

$$\rho_{total}(T) = \rho_0 + \rho_L(T) + \int_T^\infty \rho_1 f(T_k) dT_k - \int_T^\infty \rho_2 |J| \ln(T) f(T_k) dT_k \quad (6)$$

where, ρ_0 is the residual resistivity due to defect and impurity scattering, $\rho_L(T)$ is the Bloch-Gruneisen resistivity and $\rho_{\text{spin}}(T)$ is the Kondo resistivity [16].

2.3 Shape factor

Shape factor reflects the smoothness of the particle. The shape factor (Q) is defined as the mean shape of N_A measured objects according to equation (7):

$$Q = \frac{4\pi}{N_A} \sum_{i=1}^{N_A} \frac{A_i}{P_i^2} \quad (7)$$

where, A_i is the area and P_i is the perimeter length of the particles (Fig. 3).

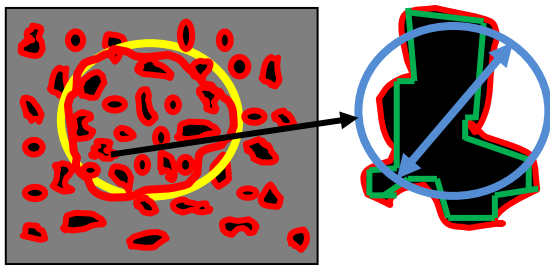


Fig. 3. Shape factor calculation [17].

Legend

	Particle area;		Particle perimeter;
	Diameter of the circle of the same area as particle		

This shape factor varies between 0 and 1. For a sphere the factor is 1 and for a cube the mean shape factor is 0,668. A value close to 1 indicates that the particle is smooth and approximately round. A value close to 0 indicates that it is elongated and rough.

The way to measure the diameter of the particle is made by marking the selected area of the particle from TEM image for performing the measurement (Fig. 4).

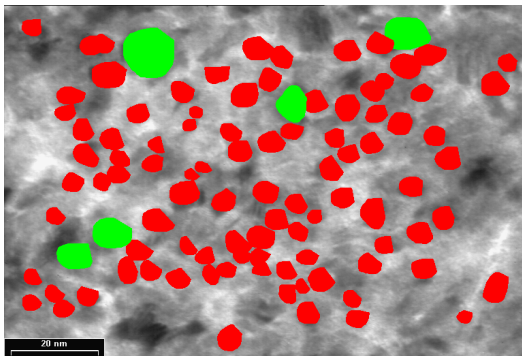


Fig. 4. Marking area selected particle from TEM image.

By determining distances between parallel lines tangent to the perimeter at opposite sides of the particle measured for angle from 15^0 to 15^0 , and making their mediation, can be calculated the diameter.

3. Results and discussion

Measurements from Fig. 5 gives a scale for the diameter of nanoparticles between (5,20 ÷ 11,78) nm and a filling factor ranges between (0,80 – 0,88). The experimentally measured (histograms) particle size distributions (in arbitrary units) plotted as functions of the particle diameter presents a maximum frequency at about 6,695 nm.

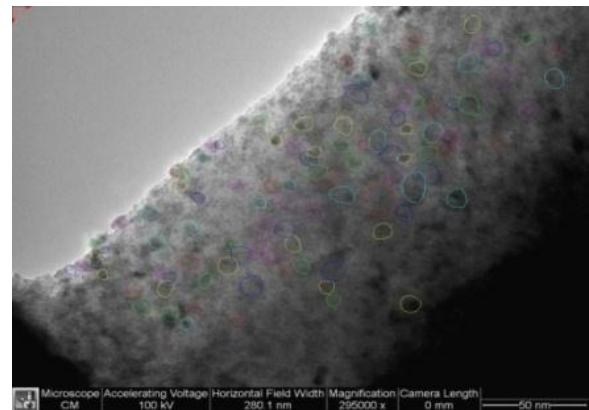
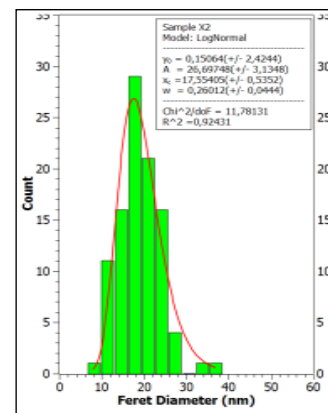


Fig. 5. The distribution of grain size for MgO-Co (sample 3) and the lognormal fit of the data.

In the case of MgO-Co sample 9, from the analysis of TEM measurements (Fig. 6), it results a scale diameter ranging between (12,80 – 27,70) nm and a filling factor estimated in the same period, (0,80 – 0,88). The distribution histogram presents a maximum frequency at about 17,554 nm.

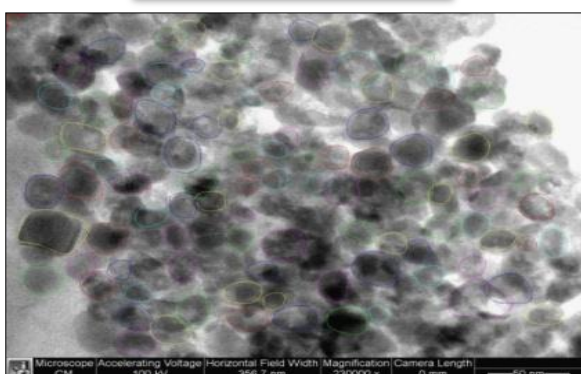
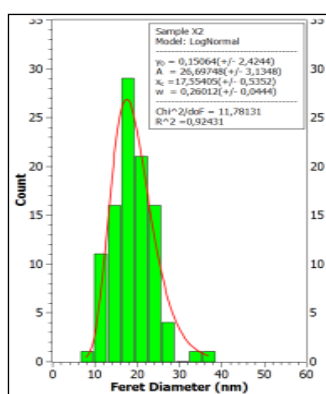


Fig. 6. The distribution of grain size for MgO-Co (sample 9) and the lognormal fit of the data.

Table 1 summarizes the parameters of particle size distribution for MgO-Co sample 3 and 9.

Table 1. The principal parameters of lognormal distribution.

sample	MgO-Co (3)	MgO-Co (9)
y_0	-1,63456 (+/-3,8855)	0,15064 (+/-2,4244)
A	37,90894 (+/-4,8492)	26,69748 (+/-3,1348)
x_c	6,69595 (+/-0,2858)	17,55405 (+/-0,5352)
w	0,33676 (+/-0,06061)	0,26012 (+/-0,0444)

4. Conclusions

In actual solid-state electronic devices, information storage or sensing devices are used multilayers technologies. The properties of this nanometer films are influenced by the microstructure as the thickness is reduced to sub-nm scale.

The mean grain size is an important feature of this films. To obtain thin films with specific properties is important to control grain size.

The present paper describes a way to determine the nanoparticle size.

EM investigation of multilayers deposited by TVA method is a good way to analyze the morphology and the grain size. The measurements present a nm-scale for the particles.

Experimental work was prepared to continue, by adding electric and magnetic measurements to conclude about future applications.

References

- [1] Y. M. Wang, J. Li, A. V. Hamza, T. W. Barbee, Jr., Ductile Crystalline-Amorphous Nanolaminates, Proc. Natl. Acad. Sci. USA **104**, 11155 (2007).
- [2] Barbee, T. W. Jr., Multilayer Synthesis by Physical Vapor Deposition, in Synthetic Modulated Structures, ed. by L. Chang and B. C. Giessen, Academic Press, New York, 313 (1985).
- [3] Barbee, T. W. Jr., Multilayer Structures: Atomic Engineering in Its Infancy, in Physics, Fabrication and Applications of Multilayered Structures, Proc. of a NATO Advanced Study Institute, New York, NY, p. 17-32 (1988).
- [4] A. Jillavenkatesa, S. J. Dapkunas, Lin-Sien Lum, Particle Size Characterization, NIST Special Publication 960-1, (2001).
- [5] N. Sivakugan N, Soil Classification, James Cook University Geoengineering lecture handout, (2000).
- [6] M. Levin, Ph. D, President S. Murphy, Vice-President, Particle Size and Shape in Pharmaceutical Applications, Metropolitan Computing Corporation (MCC), (2004).
- [7] Weixing Wang, Powder Technology, **165**, 1-10, (2006).
- [8] V. Ciupină, I. Carazeanu, G. Prodan, J. Optoelectron. Adv. Mater. **6**, 1317 (2004).
- [9] I. Carazeanu Popovici, V. Ciupină, G. Prodan, M. A. Gîrțu, J. Optoelectron. Adv. Mater. **10**(11), 2942 (2008).
- [10] L. J. Chen, J. H. Tyan, J. T. Lue, Phys. Chem. Solids **55**, 871 (1994).
- [11] G. Reiss, J. Vanca, H. Hoffmann, Phys. Rev. Lett. **56**, 2100 (1986).
- [12] T. Fujita, K. Ohshima, T. Kuroishi, J. Phys. Soc. Jpn. **40**, 90 (1976).
- [13] B. Roy, D. Chakravorty, J. Rhys. Condens. Mater. **2**, 9323 (1990).
- [14] A. Chatterjee, D. Chakravorty, Electrical, J. Mater. Sci. **27**, 4115 (1992).
- [15] J. M. Ziman, Principles of the Theory of Solids, 2nd ed., p. 224, Cambridge University Press, 1972.
- [16] J. T. Lue, Physical Properties of Nanomaterials, Encyclopedia of Nanoscience and Nanotechnology, v.X, p.1-46, (2007).
- [17] www.laboratoryequipment.com/article-particle-characterisation:tools&methods.

*Corresponding author: marinirina300@yahoo.com